Free Vibrations of Freely Supported Oval Cylinders

LARRY D. CULBERSON*
Chicago Bridge and Iron Company, Houston, Texas
AND
DONALD E. BOYD†
Oklahoma State University, Stillwater, Okla.

A study was made of the free vibration frequencies and mode shapes for freely supported oval cylindrical shells. Cross section curvatures were expressed in terms of a single eccentricity parameter that allowed a wide range of doubly symmetric ovals to be studied. Kinematic equations employing both the Love and the Donnell assumptions from thin shell theory were used in this study and results of the two formulations were compared. Little difference was observed between the results obtained from the two theories for a wide range of shell configurations. Comparisons were also made between the results obtained from this study and those from two previous approximate analyses. It was found that one of the approximate analyses (a Rayleigh-Ritz technique) was quite accurate for all ranges of eccentricities studied. The other approximate analysis (a perturbation technique) was found to be reliable for ovals with eccentricities in the range ($-0.5 \leq \epsilon \leq 0.5$). A study was also made to determine the effects of eccentricity of oval cross sections. The frequencies and mode shapes were found to vary significantly with increasing eccentricities. Irregularities in the frequency vs wave-number curves and a localized "cupping" in the region near the minimum frequency were observed. In-plane inertias were retained yielding the expected three frequencies for each combination of longitudinal and circumferential wave numbers. However, unlike the unstiffened circular cylinder, more than one set of three natural frequencies and associated mode shapes were found for some combinations of longitudinal and circumferential wave numbers. However, although the wave numbers (i.e., number of crossings) were the same in these cases, the wave shapes were obviously different.

Nomenclature

$2a,2b$ = minor and major axes of shell, respectively
A_{mn},B_{mn},C_{mn} = displacement constants
e_x,e_s,e_{xs} = axial, circumferential, and shear strain components, respectively
E = Young's modulus
h = shell thickness
k = number of terms in circumferential direction for convergence
L = 1, for Love's equations; = 0, for Donnell's equations
L_s,L_x = circumferential and longitudinal length of the shell, respectively
m,n = indices on displacement summation
$\bar{n}$ = number of full circumferential waves
r = radius of curvature
r_0 = mean radius of curvature, $L_s/2\pi$
t = time
u,v,w = orthogonal displacements
x,s,z = spatial coordinates
$[X]$ = frequency matrix
α = $(1 + \mu)/2$
β = L_s/L_x
γ = $(1 - \mu)/2$
δ_j^i = Kronecker delta
ϵ = eccentricity parameter ($|\epsilon| \leq 1$)
η = nondimensional x coordinate, x/L_x
λ = circular frequency of a noncircular cylindrical shell
μ = Poisson's ratio
ξ = nondimensional s coordinate, s/L_s
ρ = mass density
ω = nondimensional frequency of a noncircular cylindrical shell, $[\omega^2 = (1 - \mu^2)\rho L_s^2\lambda^2/E\pi^2]$
$\bar{\omega}$ = $\omega/2$

Received June 24, 1970; revision received February 2, 1971. The authors are grateful to Oklahoma State University and to the NASA Traineeship Program for funds provided to perform this study.

* Engineer, Advancement Program.
† Associate Professor, School of Mechanical and Aerospace Engineering. Associate Fellow AIAA.

Introduction

THIS paper reports on a study of the free vibration characteristics of freely supported oval cylinders. In the past years, cylindrical shells having circular cross sections have been studied very thoroughly. But many times an engineer may be called upon to design noncircular cylindrical shells. Cylindrical shells having noncircular cross sections have been used in many industrial applications; for example, in submersible and flight structures. In addition, shells designed to be circular often deviate measurably from perfect circularity once they are fabricated. This study is important because out-of-roundness may adversely affect the natural frequencies and mode shapes. Also, investigations of the free-vibration characteristics of the oval shell are necessary if the forced vibrations of oval cylindrical shells are to be studied.

For the discussions to follow, reference should be to the geometry and nomenclature of Fig. 1. The quantities ap-

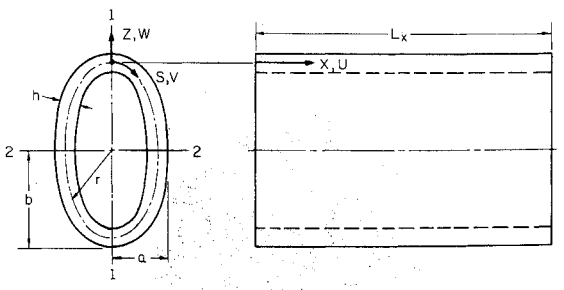

Fig. 1 Geometry of the oval shell.

pearing in Fig. 1 are defined as follows: s, x, and z are the orthogonal coordinates; v, u, and w are the corresponding displacement components; r is the variable radius of curvature; h is the shell thickness; L_x is the length of the cylindrical shell in the x direction; L_s (not shown) is the circumferential arc length of the cylindrical shell measured along the middle surface in the s direction; and $2b$ and $2a$ are the lengths of the major and minor axes of the oval cylindrical shell, respectively.

Kempner and his associates,[1,2] in considering static problems assumed a simplified, one-parameter, version of Marguerre's[3] Fourier series representation of the cylinder curvature. This curvature expression, which represents a doubly symmetric oval and approximates an ellipse having the same major-to-minor axis ratio as the oval is given as

$$1/r = (1/r_0)[1 + \epsilon \cos 4\pi s/L_s] \tag{1}$$

where ϵ is an eccentricity parameter and r_0 is a perimeter parameter. It was shown in Ref. 1 that as ϵ varies from 0 to 1 the major-to-minor axis ratio ranges from 1 to 2.06. Furthermore, to prevent negative curvatures, ϵ must obey the inequality $|\epsilon| \leq 1$. The parameter r_0 is the radius of a circular cylinder having a circumference equal to the perimeter of the oval. Thus, $r_0 = L_s/2\pi$. The full geometry of the oval is presented in Ref. 1.

Klosner,[3,5,6] using the curvature expression given by Kempner [i.e., Eq. (1)], studied the free and forced vibrations of an infinitely long oval cylindrical shell. Using equations of motion equivalent in accuracy to the Love equations for circular cylinders, Klosner assumed a frequency perturbation polynomial in the eccentricity parameter ϵ to obtain the natural frequencies and mode shapes. This procedure uncoupled the three partial differential equations of motion. The expression for the nondimensional frequency of a noncircular cylindrical shell was given as

$$\bar{P}_{il}^2 = P_{il}^2 + C_{1il}\epsilon + C_{2il}\epsilon^2 + \ldots \tag{2}$$

where i = circumferential wave numbers; l = nondimensionalized length of the longitudinal half-wave; $\bar{P}_{il}$ = nondimensional frequency of an oval with eccentricity; P_{il} = nondimensional frequency of a circular cylindrical shell of radius r_0 {i.e., $P_{il} = [(r_0^2\rho)(1 - \mu^2)p_{il}^2/E]^{1/2}$}; C_{pil} = coefficient of ϵ_p—term of the nondimensional perturbed frequency of the ilth mode; and p_{il} = natural frequency of a circular cylindrical shell of radius r_0.

Klosner found that terms higher than the third term on the right side of Eq. (2) were insignificant for $|\epsilon| \leq 0.5$. Furthermore the assumed series for the frequency led to the results that $C_{1il} = 0$. Therefore, frequencies for positive and negative ϵ were identical. The present study concluded that this approach will not yield all the free vibrational modes. This will be discussed in the sections to follow.

Theory

This development is limited to homogeneous, isotropic, elastic, thin-walled, cylindrical shells. The cross section of the shell is identified by a convex-outward, closed, plane curve resulting from the intersection of the middle surface and a plane normal to the axis of the cylinder. The sides of the shell are assumed to be at distances $z = \pm h/2$ from the middle surface, where z is measured along the normal to this surface and h is the thickness of the shell. The thickness is considered small in comparison with the longitudinal length L_x and the radius of curvature r of the middle surface.

The relations are based upon the usual Kirchhoff-Love assumptions of classical shell theory.[4,7] The strain-displacement relations used are those commonly referred to as Love's and Donnell's equations and were employed by Romano and Kempner[1,2] in analyses of noncircular cylinders. Comparisons will be made between the results obtained by these two simplifying theories. The differential equations of equilibrium follow from the application of Hamilton's principle, Ref. 7, to the freely vibrating thin cylindrical shell.

Employing Love's strain-displacement relations, Hamilton's principle yields

$$u_{xx} + \frac{(1-\mu)}{2}u_{ss} + \frac{(1-\mu)}{2}v_{xs} + \frac{\mu}{r}w_x - \frac{(1-\mu^2)}{E}\rho u_{tt} = 0 \tag{3a}$$

$$\frac{(1-\mu)}{2}v_{xx} + v_{ss} + \frac{(1+\mu)}{2}u_{xs} + \left(\frac{w}{r}\right)_s + \frac{h^2}{12}\left[\frac{(1-\mu)}{2}\frac{v_{xx}}{r^2} - \frac{w_{xxs}}{r} - \frac{w_{sss}}{r} + \frac{1}{r}\left(\frac{v}{r}\right)_{ss}\right] - \frac{(1-\mu^2)}{E}\rho v_{tt} = 0 \tag{3b}$$

$$\frac{1}{r}\left[\frac{w}{r} + v_s + \mu u_x\right] + \frac{b^2}{12}\nabla^4 w - \frac{h^2}{12}\left[\left(\frac{v_{xx}}{r}\right)_s - \left(\frac{v}{r}\right)_{sss}\right] + \frac{(1-\mu^2)}{E}\rho w_{tt} = 0 \tag{3c}$$

If the simplifying assumptions originally suggested by Donnell[8] are introduced, the equations of motion become

$$u_{xx} + \frac{(1-\mu)}{2}u_{ss} + \frac{(1+\mu)}{2}v_{xs} + \frac{\mu}{r}w_x - \frac{(1-\mu^2)}{E}\rho u_{tt} = 0 \tag{4a}$$

$$\frac{(1-\mu)}{2}v_{xx} + v_{ss} + \frac{(1+\mu)}{2}u_{xs} + \left(\frac{w}{r}\right)_s - \frac{(1-\mu^2)}{E}\rho v_{tt} = 0 \tag{4b}$$

$$\frac{1}{r}\left[\frac{w}{r} + v_s + \mu u_x\right] + \frac{h^2}{12}\nabla^4 w + \frac{(1-\mu^2)}{E}\rho w_{tt} = 0 \tag{4c}$$

where subscripts indicate differentiation.

Because the Love and Donnell equations differ only by a few terms, only the Love equations will be used in the following discussion of the formulation. Equations (3) can be rewritten in nondimensionalized form using the following dimensionless quantities:

$$\eta = x/L_x, \quad \xi = s/L_s, \quad \alpha = (1+\mu)/2, \quad \gamma = (1-\mu)/2 \tag{5}$$

$$\frac{1}{L_x^2}u_{\eta\eta} + \frac{\gamma}{L_s^2}u_{\xi\xi} + \frac{\alpha}{L_sL_x}v_{\eta\xi} + \frac{\mu}{rL_x}w_\eta - \frac{(1-\mu^2)}{E}\rho u_{tt} = 0 \tag{6a}$$

$$\frac{V_{\xi\xi}}{L_s^2} + \frac{\gamma}{L_x^2}v_{\eta\eta} + \frac{\alpha}{L_sL_x}u_{\eta\xi} + \frac{1}{L_s}\left(\frac{w}{r}\right)_\xi + \frac{h^2}{12}\left[\frac{\gamma}{L_x^2r^2}v_{\eta\eta} - \frac{1}{rL_x^2L_s}w_{\eta\eta\xi} - \frac{1}{rL_s^3}w_{\xi\xi\xi} + \frac{1}{rL_s^2}\left(\frac{v}{r}\right)_{\xi\xi}\right] - \frac{(1-\mu^2)}{E}\rho v_{tt} = 0 \tag{6b}$$

$$\frac{1}{r}\left[\frac{w}{r} + \frac{v_\xi}{L_s} + \frac{\mu}{L_x}u_\eta\right] + \frac{h^2}{12}\bar{\nabla}^4 w - \frac{h^2}{12}\left[\frac{1}{L_x^2L_s}\left(\frac{v_{\eta\eta}}{r}\right)_\xi - \frac{1}{L_s^3}\left(\frac{v}{r}\right)_{\xi\xi\xi}\right] + \frac{(1-\mu^2)}{E}\rho w_{tt} = 0 \tag{6c}$$

where

$$\bar{\nabla}^4 w = \frac{w_{\eta\eta\eta\eta}}{L_x^4} + \frac{2}{L_x^2L_s^2}w_{\eta\eta\xi\xi} + \frac{w_{\xi\xi\xi\xi}}{L_s^4}$$

The curvature expression for a doubly-symmetric oval given by Romano and Kempner[1] can be expressed nondimensionally as

$$L_s/r = 2\pi[1 + \epsilon \cos(4\pi\xi)] \tag{7}$$

For this particular problem, diplacements are assumed which satisfy the freely supported boundary conditions along the two edges $\eta = 0,1$. These conditions are

$$u_\eta = 0, \quad v = 0, \quad w = 0, \quad w_{\eta\eta} = 0 \tag{8}$$

Considering these boundary conditions, the symmetric displacements u, v, and w may be expressed nondimensionally by the following series:

$$u(\eta,\xi,t) = \sum_{m=1}^{\infty} \sum_{n=0,2}^{\infty} A_{mn} \cos m\pi\eta \cos n\pi\xi \cos\lambda t$$

$$v(\eta,\xi,t) = \sum_{m=1}^{\infty} \sum_{n=0,2}^{\infty} B_{mn} \sin m\pi\eta \sin n\pi\xi \cos\lambda t \tag{9}$$

$$w(\eta,\xi,t) = \sum_{m=1}^{\infty} \sum_{n=0,2}^{\infty} C_{mn} \sin m\pi\eta \cos n\pi\xi \cos\lambda t$$

For antisymmetric displacements the sine and cosine functions in the ξ direction are replaced by the cosine and sine functions, respectively.

Following the procedure of Refs. 1 and 2, the assumed displacements and the radius of curvature may be substituted into Love's equations to obtain three sets of coupled algebraic equations. Making this substitution and simplifying, three symmetric displacement formulas for each m and n can be written as follows:

$$[\beta^2m^2 + \gamma(2n-2)^2 - \omega^2]A_{mn} + [-\alpha\beta m(2n-2)]B_{mn} + [-\beta\mu m\epsilon(1+\delta_3{}^n)]C_{mn-2} + [-\beta\mu m(2+\epsilon\delta_2{}^n)]C_{mn} + [-\beta\mu m\epsilon]C_{mn+2} = 0 \tag{10}$$

$$A_{mn}[-\alpha\beta m(2n-2)] + B_{mn-}L_x\left[\frac{h^2\pi^2}{12L_s{}^2}\epsilon^2(1-\delta_5{}^n) \times \langle m^2\beta^2\gamma + (2n-6)^2\rangle\right] + B_{mn-}L_x\left[\frac{h^2\pi^2}{3L_s{}^2} \times \left\{(2n-2)^2\frac{\epsilon}{2}(1-\delta_3{}^n) + \frac{\epsilon}{2}(2n-6)^2(1-\frac{\epsilon}{2}\delta_4{}^n) + m^2\beta^2\gamma\left\langle\epsilon(1-\delta_3{}^n) - \frac{\epsilon^2}{4}\delta_4{}^n\right\rangle\right\}\right] + B_{mn}\left[(2n-2)^2 + \gamma\beta^2m^2 + L_x\frac{h^2\pi^2}{3L_s{}^2}\left\langle(2n-2)^2(1-\epsilon\delta_2{}^n) + \frac{\epsilon^2}{4}(2n+2)^2(1-\delta_1{}^n) + \frac{\epsilon^2}{4}(2n-6)^2 + \gamma m^2\beta^2(1 + \frac{\epsilon^2}{2} - \epsilon\delta_2{}^n - \frac{\epsilon^2}{4}\delta_3{}^n)\right\rangle - \omega^2\right] + B_{mn+2}L_x\left[\frac{h^2\pi^2}{3L_s{}^2} \times \left\langle(2n-2)^2\frac{\epsilon}{2}(1-\frac{\epsilon}{2}\delta_2{}^n) + (2n+2)^2\frac{\epsilon}{2} + m^2\beta^2\gamma\,(\epsilon - \frac{\epsilon^2}{4}\delta_2{}^n)\right\rangle\right] + B_{mn+4}L_x\left[\frac{h^2\pi^2}{12L_s{}^2}\epsilon^2\langle m^2\beta^2\gamma + (2n+2)^2\rangle\right] + C_{mn-2}\left[(2n-2)\epsilon(1+\delta_3{}^n) + L_x\frac{h^2\pi^2}{12L_s{}^2} \times \epsilon(2n-6)\langle\beta^2m^2 + (2n-6)^2\rangle\right] + C_{mn} \times \left[(2n-2)(2+\epsilon\delta_2{}^n) + L_x\frac{h^2\pi^2}{6L_s{}^2}(2n-2)(1-\frac{\epsilon}{2}\delta_2{}^n) \times \langle\beta^2m^2 + (2n-2)^2\rangle\right] + C_{mn+2}\left[(2n-2)\epsilon + L_x\frac{h^2\pi^2}{12L_s{}^2} \times \epsilon(2n+2)\langle\beta^2m^2 + (2n+2)^2\rangle\right] = 0 \tag{11}$$

$$A_{mn-2}[-\mu m\beta\epsilon(1+\delta_3{}^n)] + A_{mn}[-\mu m\beta(2+\epsilon\delta_2{}^n)] + A_{mn+2}[-\mu m\beta\epsilon] + B_{mn-2}\left[\epsilon(2n-6)(1+\delta_3{}^n) + L_x\frac{h_2\pi^2}{12L_s{}^2}(1-\delta_3{}^n)\epsilon(2n-2)\langle\beta^2m^2 - (2n-2)^2\rangle\right] + B_{mn}\left[(2n-2)(2+\epsilon\delta_2{}^n) + L_x\frac{h^2\pi^2}{6L_s{}^2}(2n-2)(1-\frac{\epsilon}{2}\delta_2{}^n) \times \langle m^2\beta^2 - (2n-2)^2\rangle\right] + B_{mn+2}\left[\epsilon(2n+2) + L_x\frac{h^2\pi^2}{12L_s{}^2} \times \epsilon(2n-2)\langle m^2\beta^2 - (2n-2)^2\rangle\right] + C_{mn+4}[\epsilon^2(1+\delta_5{}^n)] + C_{mn-2}[\epsilon(4+4\delta_3{}^n+\epsilon\delta_4{}^n)] + C_{mn}\left[(4+2\epsilon^2+\epsilon^2\delta_3{}^n + 4\epsilon\delta_2{}^n) + \frac{h^2\pi^2}{12L_s{}^2}\langle\beta^2m^2 + (2n-2)^2\rangle^2 - \omega^2\right] + C_{mn+2}[\epsilon(4+\epsilon\delta_2{}^n)] + C_{mn+4}[\epsilon^2] = 0 \tag{12}$$

where

$$\delta_j{}^i = \begin{cases} 1 & i = j \\ 0 & i \neq j \end{cases}$$

$$A_{m-n} = 0, \; B_{m-n} = 0, \; C_{m-n} = 0; \qquad n \geq 0$$

$m = 1,2,3,\ldots$; $n = 1,2,3,\ldots$.

These equations cannot be solved explicitly for A_{mn}, B_{mn}, C_{mn} because noncircularity has coupled an infinite number of equations in the ξ direction. In order to obtain a solution, the number of equations must be truncated at some n (say k) which will insure convergence to the desired accuracy. Because of the large number of equations involved, the use of a computer is essential to solve the $3k$ simultaneous equations obtained for each value of m. These equations can be written in the following matrix form:

$$\begin{bmatrix} \text{Recurrence Formula } 10 \\ \text{Recurrence Formula } 11 \\ \text{Recurrence Formula } 12 \end{bmatrix} \begin{bmatrix} A_{m1} \\ \vdots \\ A_{mk} \\ B_{m1} \\ \vdots \\ B_{mk} \\ C_{mk} \\ \vdots \\ C_{mk} \end{bmatrix} = [0] \tag{13}$$

That is,

$$[X]\begin{bmatrix} A \\ B \\ C \end{bmatrix} = [0]$$

Equation (13) requires that

$$|[\bar{X}] - \omega^2[I]| = 0 \tag{14}$$

where $[\bar{X}] = [X]$ with the ω^2 terms removed, and $[I]$ = identity matrix. The squares of the nondimensionalized natural frequencies are those values of ω^2 which satisfy Eq. (14).

The subroutine called EIGENP (see Ref. 9), modified to double precision, was used to calculate the eigenvalues (ω^2) of Eq. (14) and their corresponding eigenvectors. The eigenvectors were then used in Eqs. (9) to calculate normalized

Table 1 Nondimensional frequencies for symmetric and antisymmetric cases ($|\epsilon| = 0.50$); $L_s/L_x = 2\pi$, $h/L_s = 1/(2\pi \cdot 91.7)$, $m = 1$

$\bar{n}$	$\epsilon = 0.50$ Symmetric	$\epsilon = -0.50$ Symmetric	$\epsilon = 0.50$ Anti-symmetric	$\epsilon = -0.50$ Anti-symmetric
0	1.09797	1.09797	1.01268	1.01268
1	1.07067	0.74000	0.74000	1.07067
2	0.54898	0.54898	0.69257	0.69257
3	0.48080	0.42624	0.42624	0.48080
4	0.33789	0.33789	0.35395	0.35395
5	0.28024	0.27569	0.27569	0.28024
6	0.20638	0.20638	0.20810	0.20810
7	0.20817	0.20655	0.20655	0.20817
8	0.27003	0.27003	0.27152	0.27152
9	0.30965	0.30899	0.30899	0.30965
10	0.35630	0.35630	0.35735	0.35735
11	0.41696	0.41696	0.41696	0.41696
12	0.48658	0.48658	0.48658	0.48658
13	0.56371	0.56371	0.56371	0.56371
14	0.64779	0.64779	0.64779	0.64779

displacements. All displacements were calculated at the point of maximum displacement along the axis of the shell.

The number of points around the circumference at which the displacements were calculated was $3k - 2$. This was sufficient to insure that all sign changes in displacements would be obtained. Symmetry of the cross section allowed displacements to be calculated for only half the circumferential length.

In order to identify frequencies with mode shapes, the number of times that the displacement changed sign in half the circumferential length was counted (i.e., the number of full waves) and this was then taken to be the value of $\bar{n}$. As the eccentricity became higher this technique had to be abandoned as will be later explained.

Numerical Results

Circular shells were studied and the frequencies and mode shapes obtained for each combination of longitudinal and circumferential wave numbers compared favorably with previously known results. Having established good results for known circular shells, noncircular (oval) shells were then studied.

Table 2 Comparison of natural frequencies obtained by Sewall and by the authors

		Case 1; $a = b = 12$ in.			
m		$\bar{n}$	Sewall		Authors
		3	529.8		529.9
1		7	162.2		163.5
		10	221.3		223.3
		4	968.4		968.5
2		10	325.7		327.1
		12	361.0		362.9
		Case 2; $a = 12.95$ in., $b = 11.01$ in.			
		Symmetric		Antisymmetric	
m	$\bar{n}$	Sewall	Authors	Sewall	Authors
	3	524.1	522.0	524.2	526.3
1	7	157.1	157.8	157.0	157.8
	10	221.9	223.9	221.9	223.9
	4	956.5	954.8	956.7	957.9
2	10	310.6	310.4	310.6	310.4
	12	359.4	363.2	359.4	363.2
		Case 3; $a = 14.39$ in., $b = 9.35$ in.			
	3	491.2	459.7	492.4	521.5
1	7	138.5	129.6	138.5	131.3
	10	223.9	227.0	223.9	227.1
	4	886.1	828.2	893.0	929.4
	10	268.1	245.7	268.1	246.7
2		328.2	336.1		
	12	382.3	391.7	328.2	337.8
				382.3	393.3

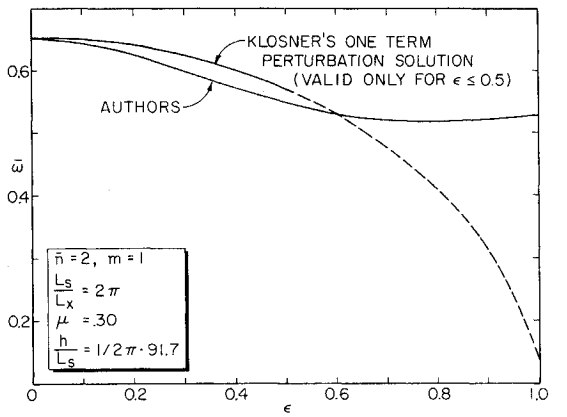

Fig. 2 Nondimensional frequency ($\bar{\omega}$) vs eccentricity ($\bar{n} = 2$, $m = 1$) Klosner and the authors.

Because in-plane inertias were retained in this study, three natural frequencies were associated with each combination of longitudinal and circumferential wave number. Usually, however, the "first-frequency" (i.e., the lowest of the three found for each combination of wave numbers) is of most interest to designers. Therefore, most of the results of this study pertain to the first frequencies and their associated mode shapes.

A computer program was written to facilitate the solution of frequency equations derived by Klosner.[6] First frequencies obtained from this program and the authors' results using Love's equations were compared at the lowest first frequency for $m = 1$ and the following parameters:

$$L_s/L_x = 2\pi,\ h/L_s = 0.0017356,\ \mu = 0.30$$

For the accuracy desired, convergence was obtained with $k =$

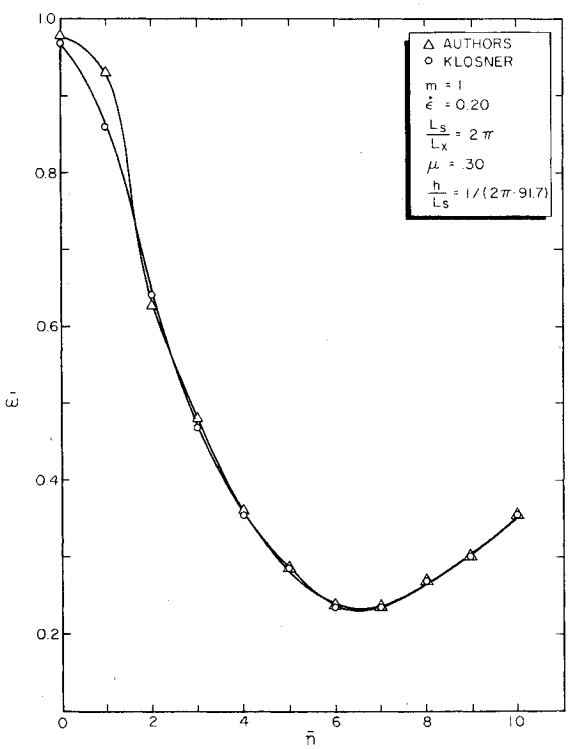

Fig. 3 Nondimensional frequency ($\bar{\omega}$) vs mode number $\bar{n}$ ($\epsilon = 0.20$) Klosner and the authors.

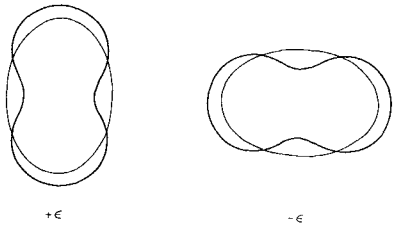

Fig. 4 Typical ($\bar{n}$ = 2) doubly symmetric mode shapes for ± ϵ.

21 (i.e., with 21 terms in the circumferential direction). Very good comparisons with Klosner's perturbation technique of calculated frequencies were observed for values of ϵ where that technique is valid, as is illustrated by Fig. 2. Figure 3 compares the variation of the frequency with mode number $\bar{n}$ for modes symmetric about the vertical axis (axis 1-1 in Fig. 1) and for $\epsilon = 0.2$.

Table 1 shows that for symmetric displacements with $\bar{n}$ = 2,4,6,8,..., identical frequencies were found for $\pm\epsilon$. Also, for antisymmetric displacements with $\bar{n}$ = 2,4,6,8... identical frequencies were found for $\pm\epsilon$. However, frequencies obtained for symmetric displacements with $\bar{n}$ = 1,3,5,7... and negative ϵ were identical to the frequencies obtained for antisymmetric displacements with $\bar{n}$ = 1,3,5,7 and positive ϵ.

An explanation of these observations is in order. Changing the sign of ϵ corresponds to a rigid body rotation of the oval through 90°. As illustrated by Fig. 4, the doubly symmetric mode shapes are identical for $\pm\epsilon$. However, mode shapes which are symmetric about the vertical axes and antisymmetric about the horizontal axes (i.e., singly symmetric) do not possess identical natural frequencies for $\pm\epsilon$ and identical wave numbers $\bar{n}$. This is explained by considering a typical singly symmetric mode (Fig. 5) for $\pm\epsilon$. Although the wave number ($\bar{n}$) is the same for $\pm\epsilon$, the displaced configurations (hence, the natural frequencies) are not identical. It is therefore necessary to include both symmetric and antisymmetric displacement functions in a parametric investigation limited to $0 \leq \epsilon \leq 1$.

Sewall[10] studied both theoretically and experimentally the natural frequencies of freely supported elliptical shells using a Rayleigh-Ritz technique and numerical integration of the associated energy integrals. Table 2 compares natural frequencies calculated for a 6061 aluminum cylinder having the following characteristics:

$$L_s = 75.4\,\text{in.} \quad L_x = 24.0\,\text{in.} \quad h = 0.032\,\text{in.}$$

$$E = 10^7\,\text{psi} \quad \mu = 0.30 \quad \rho = 2.588(10^{-4})\,\text{lb-sec}^2/\text{in.}^4$$

Three different cross section shapes were studied—case 1: $a = b = 12$ in. ($\epsilon = 0.0$); case 2: $a = 12.95$ in., $b = 11.01$ in. ($\epsilon = -0.24236$); case 3: $a = 14.39$ in., $b = 9.35$ in. ($\epsilon = -0.62706$).

Good comparisons were observed between the results of the elliptical and oval shells for case 1 ($\epsilon = 0.0$); the greatest deviation being 0.9%. For case 2 ($\epsilon = -0.24236$) the frequencies obtained for the oval cross-section deviate from −0.4% to +0.8% from those of the ellipse. For case 3 ($\epsilon = -0.62806$) the frequencies obtained for the oval deviate from −9.1% to +5.9%. Errors increase as the eccentricity increases because the oval deviates more from the ellipse as ϵ increases. But the results are good, considering

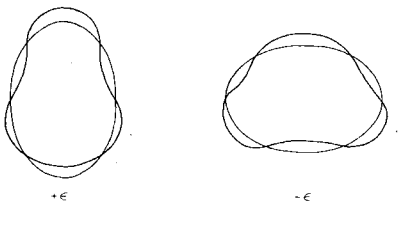

Fig. 5 Typical ($\bar{n}$ = 3) singly symmetric mode shapes for ± ϵ.

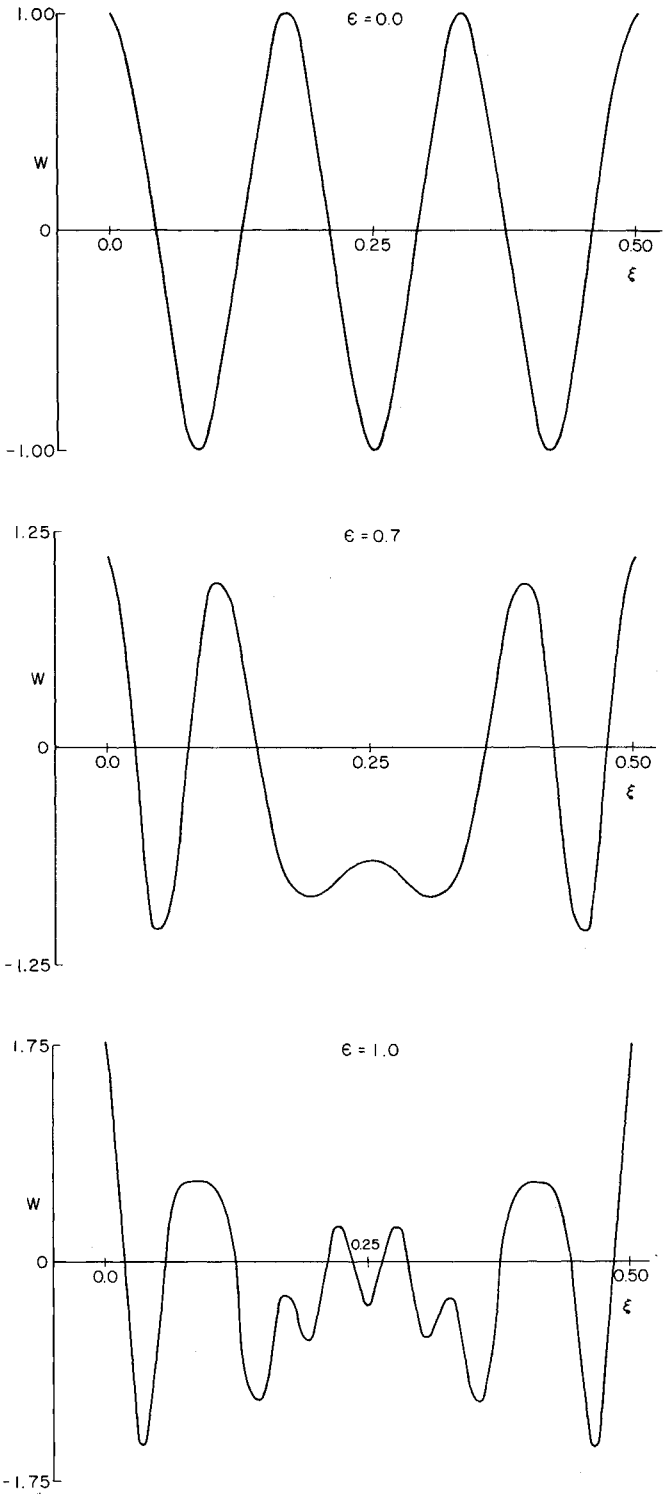

Fig. 6 Mode shapes ($\bar{n}$ = 6, m = 3).

that Sewall used an elliptical cylinder whereas the authors used an approximating oval cylinder.

It should be noted in Table 2 that for case 3, $m = 2$, there are two first-frequencies for $\bar{n} = 10$ in the symmetric case, and two for $\bar{n} = 12$ in the antisymmetric case. Coupling of terms in the displacement series results in modes which represent a superposition of all terms. Furthermore, there may develop two (or more) modes which have the same number of crossings (i.e., full waves) around the circumference. In general, these modes correspond to different first frequencies. Therefore, the conventional manner of describing modes by the number of crossings was judged to be no longer adequate. The authors have adopted the method of tracing the calcu-

lated modes through a range of ϵ from 0 to 1, and referring to the mode by the number of crossings which that mode possessed for $\epsilon = 0$. This number would identify the wave regardless of the number of crossings it may acquire for higher ϵ. Figures 6 and 7 illustrate the development of wrinkles and subsequent crossings as ϵ is increased from zero. This method of identifying modes has the advantage of unique definition of each mode.

A detailed study was made of oval shells having constant longitudinal and circumferential lengths and thicknesses. This study was restricted to a thorough investigation of the symmetric modes for only positive values of the eccentricity parameter ϵ. The restriction was made because of computer time. Love's equations were used in this study. The eccentricity parameter (ϵ) was varied from 0 to 1, the longitudinal mode m from 1 to 4, and the circumferential mode $\bar{n}$

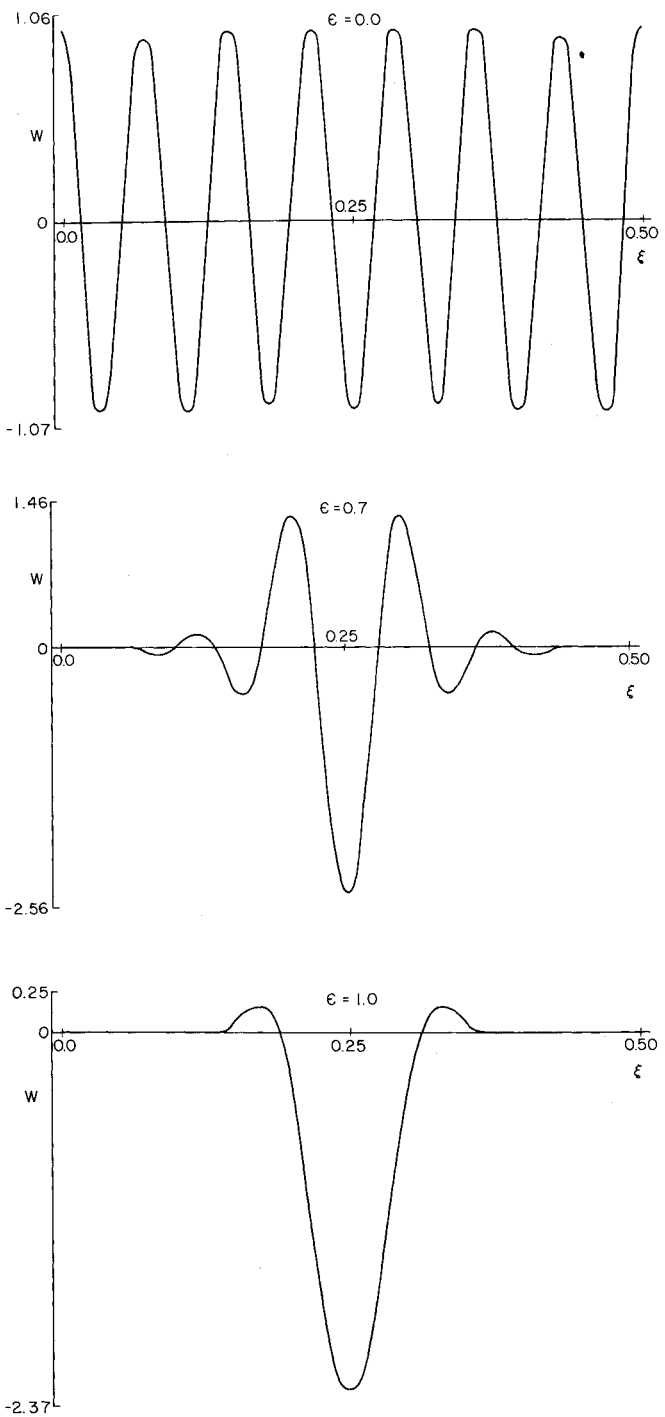

Fig. 7 Mode shapes ($\bar{n} = 14$, $m = 4$).

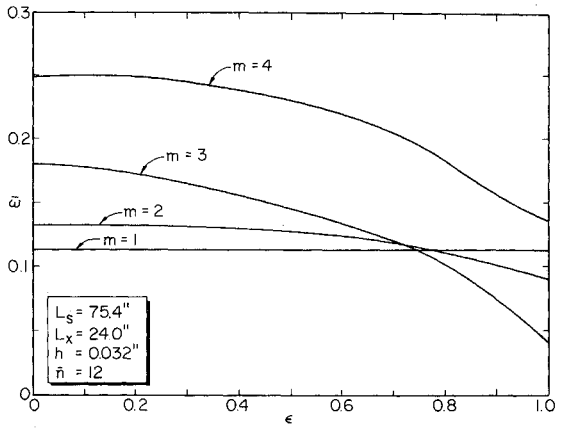

Fig. 8 Nondimensional frequency ($\bar{\omega}$) vs eccentricity ($\bar{n} = 12$).

from 0 to 12 and 16. ($\bar{n}$ varied between 12 and 16 in order to include the lowest frequency and a few of the higher frequencies near this lowest value of $\bar{\omega}$.) It was desired to use higher values of m, but due to computer space and time limitations, $m = 4$ was the largest feasible value. For the accuracy desired, adequate convergence for $m = 1$ to 3 was attained with $k = 25$; for $m = 4$, $k = 27$.

Figure 8 shows the frequency ($\bar{\omega}$) variation with eccentricity ϵ and mode number m for one value of $\bar{n}$ ($\bar{n} = 12$). Contrary to circular cylinder behavior, as the value of m increases the frequencies ($\bar{\omega}$) decrease (for higher ϵ).

The frequency ($\bar{\omega}$) variation with the mode numbers $\bar{n}$ and m is shown for $\epsilon = 0.5$ in Fig. 9. As the value of eccentricity (ϵ) increases, the curves become more irregular. This irregularity can be partially attributed to the symmetric forms being studied. If the value of ϵ is less than zero (in which case the modes are all symmetric about axis 2-2 in Fig. 1, instead of axis 1-1), most of this irregularity is erased. For small $\bar{n}$,

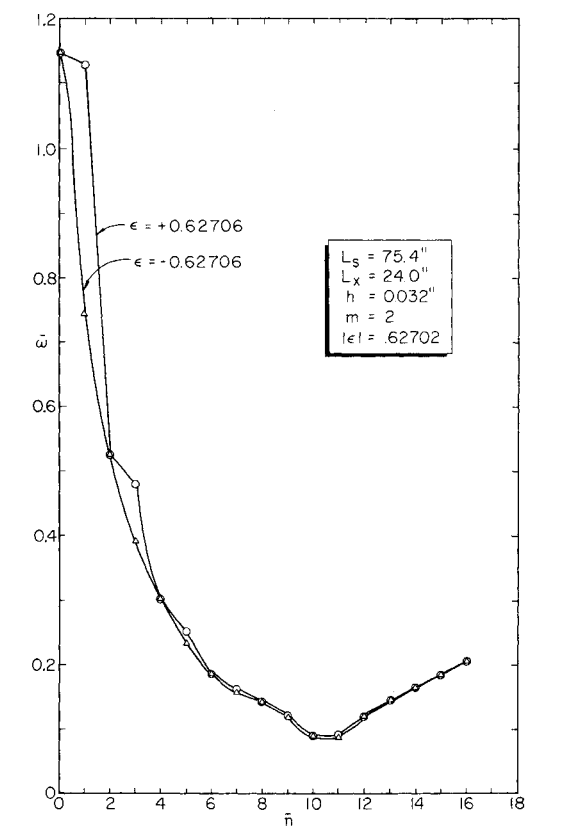

Fig. 9 Symmetric nondimensional frequency ($\bar{\omega}$) vs mode number $\bar{n}$ ($\epsilon = 0.50$).

Table 3 Comparison of the nondimensional frequencies ($\bar{\omega}$) obtained by the Love and Donnell equations; $m = 3$, $\epsilon = 1.0$, $h = 0.032$ in., $L_s = 75.4$ in.

β	3.14		1.0		0.20		0.10	
$\bar{n}$	Love	Donnell	Love	Donnell	Love	Donnell	Love	Donnell
0	1.50920	1.50921	0.88741	0.88741	0.17748	0.17748	0.08874	0.08874
1	1.50824	1.50824	0.67817	0.67817	0.06392	0.06390	0.01749	0.01741
2	0.74333	0.74336	0.22727	0.22727	0.00658	0.00656	0.00338	0.00326
3	0.74095	0.74098	0.18082	0.18083	0.00961	0.00954	0.00674	0.00660
4	0.42602	0.42607	0.09001	0.09002	0.01696	0.01686	0.01205	0.01193
5	0.42253	0.42259	0.08053	0.08054	0.01958	0.01951	0.01875	0.01871
6	0.28144	0.28154	0.01850	0.01850	0.02742	0.02738	0.02718	0.02714
7	0.27809	0.27820	0.03218	0.03219	0.03729	0.03726	0.03717	0.03714
8	0.23937	0.23946	0.05838	0.05838	0.04880	0.04877	0.04872	0.04869
9	0.22370	0.22378	0.06950	0.06951	0.06186	0.06185	0.06180	0.06178
10	0.16828	0.16830	0.08197	0.08197	0.07648	0.07647	0.07642	0.07641
11	0.07261	0.07262	0.09709	0.09710	0.09264	0.09263	0.09259	0.09258
12	0.04204	0.04204	0.11355	0.11356	0.11035	0.11034	0.11029	0.11028
13	0.14033	0.14034	0.13218	0.13218	0.12959	0.12958	0.12954	0.12953
14	0.11674	0.11674	0.15261	0.15262	0.15037	0.15036	0.15032	0.15031
15	0.18779	0.18782	0.17473	0.17474	0.17270	0.17269	0.17264	0.17264

the odd mode-number frequencies are lower for $-\epsilon$ than for $+\epsilon$, but converge to the same value as $\bar{n}$ increases. Also, in the region surrounding the lowest frequency a "cupping" effect is encountered. This local effect becomes more apparent as the eccentricity increases.

To compare the Love and Donnell equations, frequencies were obtained by both sets of equations for a range from a relatively short shell ($\beta = 3.14$) to a relatively long shell ($\beta = 0.10$).

As is evident from Table 3, the Love and Donnell equations give almost identical results for this range of shell parameters. The Donnell equations provided slightly higher frequencies for shorter shells and slightly lower frequencies for longer shells. Because it was not the specific objective of this study to compare frequencies obtained by the Love and Donnell equations, the ratio L_s/L_x was the only parameter varied. However, these results seem to indicate that the Donnell equations are comparatively accurate.

Conclusions

A method has been presented to determine the natural frequencies and mode shapes of freely supported doubly symmetric oval cylindrical shells. Oval shells were investigated and the following observations were made.

1) Frequencies obtained for oval cylinders with low eccentricities compared favorably with results obtained by Sewall[10] for ellipses with corresponding ratios of b/a. As the eccentricity increased, the results were less favorable. For a deviation of no more than 10%, the maximum allowable value of eccentricity is about 0.65.

2) Frequencies obtained in this study compared favorably with those obtained by the perturbation technique of Klosner in the range where that technique is valid ($\epsilon \leq 0.5$).

3) As the longitudinal modes (m) were increased, the number of circumferential terms (k) had to be increased to obtain accurate frequencies and mode shapes. To obtain a minimum accuracy of three significant numbers for the normalized displacements, k was taken to be 25 for values of $m \leq 3$, and 27 for $m = 4$.

4) For higher $\bar{n}$, as the eccentricity increased it was found that the frequencies for increasing values of m decreased to a point, then increased.

5) As the eccentricity increased, curves of frequency vs $\bar{n}$ became highly irregular. This was partially due to the symmetric forms (axis 1-1 in Fig. 1) studied. Frequencies obtained for modes symmetric about axis 2-2 in Fig. 1 erased the greater percentage of this irregularity.

6) Identical frequencies were obtained for $\pm\epsilon$ for even values of $\bar{n}$. Different frequencies were obtained for $\pm\epsilon$ for odd values of $\bar{n}$. However, as $\bar{n}$ increased, the two values converged.

7) As the eccentricity increased, the mode shapes varied significantly from those of the circular cases. This was interpreted physically as being due to localized bending in the flatter regions of the oval cylinders; mathematically, to coupling of terms in the solution functions.

8) The Love and Donnell equations gave nearly identical results for noncircular cylinders for the range of shell parameters studied.

References

[1] Romano, F. and Kempner, J., "Stress and Displacement Analysis of a Simply Supported, Noncircular Cylindrical Shell under Lateral Pressure," PIBAL Rept. 415, July 1958, Polytechnic Inst. of Brooklyn.

[2] Romano, F. and Kempner, J., "Stresses in Short Noncircular Cylindrical Shells under Lateral Pressure," *Transactions of the ASME, Ser. E: Journal of Applied Mechanics*, Vol. 29, Dec. 1962, pp. 669–674.

[3] Marguerre, K., "Stabilitat der Zylindershale ver nderlicher Krummung," TM 1302, July 1951, NACA.

[4] Kempner, J., "Energy Expressions and Differential Equations for Stress and Displacement Analyses of Arbitrary Cylindrical Shells," PIBAL Rept. 371, April 1957, Polytechnic Inst. of Brooklyn.

[5] Klosner, Jerome M., "Frequencies of an Infinitely Long Noncircular Cylindrical Shell, Part II," PIBAL Rept. 552, Dec. 1959, Polytechnic Inst. of Brooklyn.

[6] Klosner, J. M., "Free and Forced Vibrations of a Long Noncircular Cylindrical Shell," PIBAL Rept. 561, Sept. 1960, Polytechnic Inst. of Brooklyn.

[7] Kraus, H., *Thin Elastic Shells*, Wiley, New York, 1967.

[8] Donnell, L. H., "Stability of Thin-Walled Tubes under Torsion," Rept. 479, 1934, NACA.

[9] Grad, J. and Brebner, M. A., "Eigenvalues and Eigenvectors of a Real General Matrix," *Communications of the ACM*, Vol. 11 No. 12, Dec. 1968, pp. 820–826.

[10] Sewall, J. L., Thompson, W. M. Jr., Pusey, C. G. "An Experimental and Analytical Vibration Study of Elliptical Cylindrical Shells", TN D-6089, Feb. 1971, NASA.